

# Consequences on variable $\Lambda$ -models from distant Type Ia supernovae and compact radio sources

R. G. Vishwakarma

IUCAA, Post Bag 4, Ganeshkhind, Pune 411 007, India

E-mail: vishwa@iucaa.ernet.in

**Abstract.** We study the magnitude-redshift relation for the Type Ia supernovae data and the angular size-redshift relation for the updated compact radio sources data (from Gurvits et al) by considering four variable  $\Lambda$ -models:  $\Lambda \sim S^{-2}$ ,  $\Lambda \sim H^2$ ,  $\Lambda \sim \rho$  and  $\Lambda \sim t^{-2}$ .

It is found that all the variable  $\Lambda$ -models, as well as the constant  $\Lambda$ -Friedmann model, fit the supernovae data equally well with  $\chi^2/\text{dof} \approx 1$  and require non-zero, positive values of  $\Lambda$  and an accelerating expansion of the universe. The estimates of the density parameter for the variable  $\Lambda$ -models are found higher than those for the constant  $\Lambda$ -Friedmann model.

From the compact radio sources data, it is found, by assuming the no-evolution hypothesis, that the Gurvits et al' model (Friedmann model with  $\Lambda = 0$ ) is not the best-fitting model for the constant  $\Lambda$  case. The best-fitting Friedmann model (with constant  $\Lambda$ ) is found to be a low density, vacuum-dominated accelerating universe. The fits of this data set to the (variable, as well as, constant  $\Lambda$ -) models are found very good with  $\chi^2/\text{dof} \approx 0.5$  and require non-zero, positive values of  $\Lambda$  with either sign of the deceleration parameter. However, for realistic values of the matter density parameter, the only interesting solutions are (a) estimated from the supernovae data: the best-fit solutions for the flat models (including the constant  $\Lambda$  case); (b) estimated from the radio sources data: the global best-fit solutions for the models  $\Lambda \sim H^2$  and  $\Lambda \sim \rho$ , the best-fit solution for the flat model with  $\Lambda = \text{constant}$  and the Gurvits et al' model.

It is noted that, as in the case of recent CMB analyses, the data sets seem to favour a spherical universe ( $k > 0$ ).

PACS numbers: 04.20.Jb, 98.80.Es

## 1. Introduction

The cosmic distance measures, for example, the *luminosity distance* and the *angular size distance*, depend sensitively on the spatial curvature and the expansion dynamics of the models and consequently on the parameters of the models. For this reason, the magnitude-redshift ( $m$ - $z$ ) relation for a distant *standard candle* and the angular size-redshift ( $\Theta$ - $z$ ) relation for a distant *standard measuring rod* have been proposed as potential tests for cosmological models and play crucial role in determining cosmological parameters.

The observations on magnitude and redshift of Type Ia supernovae made, independently, by Perlmutter et al (1999) and Riess et al (1998) appear to suggest that our universe may be accelerating with a large fraction of the cosmological density in the form of the cosmological  $\Lambda$ -term. Their findings arise from the study of more than 50 Type Ia supernovae with redshifts in the range  $0.16 \leq z \leq 0.83$  and suggest Friedmann models with negative pressure-matter such as a cosmological constant, domain walls or cosmic strings (Vilenkin 1985, Garnavich et al 1998).

On the other hand, models with a dynamic cosmological term  $\Lambda(t)$  has been considered in numerous papers to explain the observed small value of  $\Lambda$ , which is about 120 orders of magnitude below the value for the vacuum energy density predicted by quantum field theory (Wienberg 1989, Carroll et al 1992, Sahni and Starobinsky 2000). It has been argued that, due to the coupling of the dynamic degree of freedom with the matter fields of the universe,  $\Lambda$  relaxes to its present small value through the expansion of the universe and the creation of photons. This approach is essentially phenomenological in nature but explains, in a natural way, the present small value of  $\Lambda$  which might be large in the early universe. From this point of view, the cosmological constant is small because the universe is old.

As the dynamics of the variable  $\Lambda$ -models depends sensitively on the chosen dynamic law for the variation of  $\Lambda$  and, in general, becomes altogether different from the dynamics of the corresponding constant  $\Lambda$ -models, there is no reason to believe that the observations of distant objects would also agree with the variable  $\Lambda$ -models, given that they agree with the corresponding constant  $\Lambda$ -ones, especially for the same estimates of the parameters. In this view, it would be worth while to test the consistency of these observations with the variable  $\Lambda$ -models and find the estimates of different cosmological parameters required by these models.

In this paper, we consider the data on the magnitude and redshift of

Type Ia supernovae from Perlmutter et al and the data on the angular size and redshift of compact radio sources updated and extended recently by Gurvits et al (1999) and study the  $m$ - $z$  and the  $\Theta$ - $z$  relations in some decaying  $\Lambda$ -models. For this purpose, we consider the following four cases of the phenomenological decay of  $\Lambda$ :

- case (1):  $\Lambda \sim S^{-2}$ ,
- case (2):  $\Lambda \sim H^2$ ,
- case (3):  $\Lambda \sim \rho$ ,
- case (4):  $\Lambda \sim t^{-2}$ ,

where  $S$ ,  $H$ ,  $\rho$  and  $t$  are, respectively, the scale factor of the R-W metric, the Hubble parameter, the energy density and the cosmic time. These are among the main dynamical laws one finds in the literature proposed for the decay of  $\Lambda$ . Case (1), which has been the subject of most attention (Ozer and Taha 1987; Chen and Wu 1990; Abdel-Rahman 1992; Abdussattar and Vishwakarma 1996, 1997; to mention a few), was originally proposed by Chen and Wu through dimensional arguments made in the spirit of quantum cosmology. It is interesting that this ansatz also comes out as a natural consequence of incorporating the contracted Ricci-collineation along the fluid flow vector in the Friedmann model (Abdussattar and Vishwakarma 1996; Vishwakarma 1999, 2000a).

The case (2) has been proposed from the similar dimensional arguments as made by Chen and Wu (Carvalho et al 1992, Waga 1993) and also from other arguments (Lima and Carvalho 1994) and has also been considered by several other authors, e.g., Salim and Waga (1993), Arbab and Abdel-Rahman (1994), Wetterich (1995), Arbab (1997). In view of the present estimates of  $\Lambda$  being of the order of  $H_0^2$ , this ansatz seems as a natural dynamic law for the decay of  $\Lambda$ . (The subscript zero denotes the value of the quantity at the present epoch).

The dynamical law mentioned in the case (3) has been obtained on the dimensional ground by suggesting that  $\Lambda \sim \Omega H^2$  which leads to  $\Lambda \sim \rho$ , (Vishwakarma 2000b), where  $\Omega$  is the density of the matter in units of the critical density, i.e.,  $\Omega \equiv \rho/\rho_c = 8\pi G\rho/3H^2$  (note that in our notation,  $\Omega$  has contributions from baryons, neutrinos, radiation, etc. and dark matter *but not from*  $\Lambda$ ).

The case (4) has also been considered by several authors by imposing supplementary conditions which are equivalent to assuming a power law for the scale factor (Endo and Fukui 1977, Lau 1985, Bertolami 1986, Berman

and Som 1990, Berman 1991, Beesham 1994, Lopez and Nanopoulos 1996).

## 2. General Features of the models

In order to find the dynamics of the models resulting from the four cases of  $\Lambda$  mentioned above and then to compare our results with the earlier works, we consider the homogeneous and isotropic models in Einstein's theory. We assume that the matter source in the universe is described by the perfect fluid energy momentum tensor

$$T^{ij} = (\rho + p)u^i u^j + p g^{ij}, \quad (1)$$

where  $\rho$  is the density of baryons, plus neutrinos, plus radiation, etc., plus dark matter. The Einstein field equations are, then, given by

$$R^{ij} - \frac{1}{2} R g^{ij} = -8\pi G \left[ T^{ij} - \frac{\Lambda(t)}{8\pi G} g^{ij} \right]. \quad (2)$$

For simplicity we consider units with  $c = 1$ . In view of the Bianchi identities, this equation suggests that  $\Lambda$  would become constant for  $T^{ij} = 0$ . Also,  $\Lambda$  must be a constant if  $T^{ij}$  is conserved separately (we consider  $G$  as a true constant). This implies that existence of some non-vanishing matter, however small, is necessary to kick  $\Lambda$  to start varying. In this connection, we recall that a decaying  $\Lambda$  has led to the possibility of non-singular models in which initially all the energy is locked up in potential form in the curvature of spacetime and as the universe evolves, curvature unfolds and creates matter (Ozer and Taha 1987, Abdussattar and Vishwakarma 1996). In this view, this primordial tiny matter (required by a decaying  $\Lambda$ ) in the otherwise empty baby universe might serve the purpose of primordial seeds for structure formation.

We also observe from equation (2) that the conserved quantity is now  $[T^{ij} - \{\Lambda(t)/8\pi G\}g^{ij}] \equiv T_{\text{total}}^{ij}$  and not  $T^{ij}$  and  $\Lambda$  separately as would have been the case, had  $\Lambda$  remained a true constant. Thus the incorporation of a variable  $\Lambda$  in the Einstein field equations is equivalent to postulating an additional source  $-(\Lambda/8\pi G)g^{ij} \equiv T_v^{ij}$  as the energy momentum tensor of vacuum with the energy density of vacuum  $\rho_v = -p_v = \Lambda/8\pi G$ .

For the Robertson-Walker metric

$$ds^2 = -dt^2 + S^2(t) \left\{ \frac{dr^2}{1 - kr^2} + r^2(d\theta^2 + \sin^2 \theta d\phi^2) \right\} \quad (3)$$

and the usual barotropic equation of state of the matter source

$$p = w\rho, \quad 0 \leq w = \text{constant} \leq 1, \quad (4)$$

equation (2) yields the following two independent equations: the Friedmann equation

$$\frac{\dot{S}^2}{S^2} + \frac{k}{S^2} = \frac{8\pi G}{3}\rho + \frac{\Lambda}{3} \quad (5)$$

and the Raychaudhuri equation

$$-\frac{\ddot{S}}{S} = \frac{4\pi G}{3}(1 + 3w)\rho - \frac{\Lambda}{3}. \quad (6)$$

It is common in cosmology to consider the constant  $w = 1/3$  for the radiation-like case and  $w = 0$  for the dust-like case. Recently  $-1 < w < 0$  has been suggested by postulating an ‘x-fluid’ (Turner and White 1997, Zlatev et al 1999) to make up the long-sought dark matter. However, these new species of matter with negative pressure are equivalent to a variable cosmological term and will not be considered here. The divergence of equation (2) leads to

$$\dot{\rho}_{\text{tot}} + 3(\rho_{\text{tot}} + p_{\text{tot}})\frac{\dot{S}}{S} = 0, \quad (7)$$

where  $\rho_{\text{tot}} = \rho + \rho_v$  and  $p_{\text{tot}} = p - \rho_v$ . Equation (7) can also be written as

$$\rho = CS^{-3(1+w)} - \frac{S^{-3(1+w)}}{8\pi G} \int \dot{\Lambda} S^{3(1+w)} dt, \quad C = \text{constant}. \quad (8)$$

This indicates that a decaying  $\Lambda$  ( $\dot{\Lambda} < 0$ ) makes a positive contribution to  $\rho$ . Equations (5) and (6) can be used to obtain

$$2\frac{\ddot{S}}{S} + (1 + 3w) \left( \frac{\dot{S}^2}{S^2} + \frac{k}{S^2} \right) - (1 + w)\Lambda = 0, \quad (9)$$

which gives the dynamics of the scale factor for a particular  $\Lambda$ .

We shall now describe, briefly, the models resulting from the different dynamical laws for the decay of  $\Lambda$  mentioned in the previous section.

**Case (1):**

We consider

$$\Lambda = \frac{n_1}{S^2}, \quad (10)$$

where the constant  $n_1$  is a new cosmological parameter replacing the original  $\Lambda$  and is to be determined from the observations. Equations (8), (9) and (10) give the dynamics of the model as

$$\rho = C_1 S^{-3(1+w)} + \frac{n_1 S^{-2}}{4\pi G(1+3w)}, \quad C_1 = \text{constant} \quad (11)$$

and

$$\dot{S}^2 = \frac{8\pi G C_1}{3} S^{-(1+3w)} + \frac{n_1(3+w)}{3(1+w)} - k. \quad (12)$$

**Case (2):**

We now consider

$$\Lambda = n_2 H^2, \quad (13)$$

where, as in the previous case, the parameter  $n_2$  is to be determined from the observations. The use of (13) in equations (5) and (8), leads to the following equations

$$\rho = C_2 S^{(n_2-3)(1+w)} - \frac{n_2 k S^{-2}}{4\pi G[(3-n_2)(1+w)-2]}, \quad C_2 = \text{constant} \quad (14)$$

and

$$\dot{S}^2 = \frac{8\pi G C_2}{(3-n_2)} S^{(n_2-3)(1+w)+2} - \frac{(1+3w)k}{[(3-n_2)(1+w)-2]}, \quad (15)$$

which determine the dynamics of the model.

**Case (3):**

We now consider the case

$$\Lambda = n_3 \rho, \quad (16)$$

where the parameter  $n_3$ , describing the model, is to be determined from the observations as in the earlier cases (1) and (2).

The dynamics of the models can be obtained from equations (5), (8) and (16) as

$$\rho = C_3 S^{-3(1+w)/(1+n)}, \quad C_3 = \text{constant} \geq 0 \quad (17)$$

and

$$\dot{S}^2 = \frac{8\pi G C_3}{3} (1+n) S^{(2n-1-3w)/(1+n)} - k, \quad (18)$$

where  $n \equiv n_3/8\pi G$ .

#### Case (4):

Finally we consider the case

$$\Lambda = \frac{n_4}{t^2}, \quad (19)$$

where the parameter  $n_4$  describes this family of models. By using (19), equation (9) can be written as

$$\frac{\ddot{x}}{x} = \frac{3(1+w)^2 n_4}{4t^2}, \quad (20)$$

where the new variable  $x$  is related to  $S$  by means of the transformation

$$\frac{\dot{S}}{S} = \frac{2}{3(1+w)} \frac{\dot{x}}{x} \quad (21)$$

implying that  $S \sim x^{2/3(1+w)}$ . Here we have restricted ourselves to the flat model only as has been done by the other authors. By assuming  $t = e^y$ , equation (20) can be further transformed to

$$\frac{d^2 x}{dy^2} - \frac{dx}{dy} - \frac{3(1+w)^2 n_4}{4} x = 0, \quad (22)$$

which gives a physically viable solution as

$$S \sim t^{n_5}, \quad \text{with } n_5 = \frac{1 + \sqrt{1 + 3(1+w)^2 n_4}}{3(1+w)}, \quad (23)$$

provided  $n_4 > -1/3(1+w)^2$ . Other solutions (for  $n_4 \leq -1/3(1+w)^2$ ) are not interesting on the ground of age considerations (Overduin and Cooperstock 1998). Solution (23) is consistent with the different power-law solutions obtained by various authors by assuming different supplementary conditions, as we have mentioned in the previous section. However, in view of  $H \sim t^{-1}$  as is implied by equation (23), this case reduces to the case (2) of  $\Lambda \sim H^2$  and will not be considered separately further.

While comparing the models with observations, we shall be mostly interested in the effects which occurred at redshift  $z < 5$ . We, therefore, neglect radiation and consider  $w = 0$  in the following. Equations (5) and (6), then, can be recast in the following forms to give the relative contributions of different cosmological parameters at the present epoch:

$$1 + \Omega_{k0} = \Omega_0 + \Omega_{\Lambda 0}, \quad (24)$$

$$2[q_0 + \Omega_{\Lambda 0}] = \Omega_0, \quad (25)$$

where  $\Omega_{\Lambda} \equiv \Lambda/3H^2$  and  $\Omega_k \equiv k/S^2 H^2$  are, respectively, the energy density of vacuum and that associated with curvature in units of the critical density and  $q$  is the deceleration parameter.

It would be worth while to find out if there exist some characteristics of the models, other than the different dependences of  $\Lambda$ , which clearly distinguish the evolution of the models discussed above. The dynamics of the models, described by equations (12), (15) and (18), depend on the parameters  $n_i$  and  $C_i$ . In order to make the comparison possible, we write them in terms of  $H_0$ ,  $\Omega_0$  and  $\Omega_{\Lambda 0}$  as follows:

$$n_1 = 3H_0^2 S_0^2 \Omega_{\Lambda 0}, \quad C_1 = \frac{3H_0^2}{8\pi G} [\Omega_0 - 2\Omega_{\Lambda 0}] S_0^3; \quad (26)$$

$$n_2 = 3\Omega_{\Lambda 0}, \quad C_2 = \frac{3H_0^2}{8\pi G} \left[ \frac{(1 - \Omega_{\Lambda 0})(\Omega_0 - 2\Omega_{\Lambda 0})}{1 - 3\Omega_{\Lambda 0}} \right] S_0^{3(1-\Omega_{\Lambda 0})}; \quad (27)$$

$$n_3 = 8\pi G \frac{\Omega_{\Lambda 0}}{\Omega_0}, \quad C_3 = \frac{3H_0^2}{8\pi G} \Omega_0 S_0^{3\Omega_0/(\Omega_0 + \Omega_{\Lambda 0})}, \quad (28)$$

where  $S_0 = H_0^{-1} \sqrt{k/\Omega_{k0}}$  with  $\Omega_{k0}$  given by equation (24). Equations (12), (15) and (18) then reduce, respectively, to the following.

$\Lambda \sim S^{-2}$ :

$$\dot{S}^2 = H_0^2 S_0^2 \left[ (\Omega_0 - 2\Omega_{\Lambda 0}) \frac{S_0}{S} + (1 - \Omega_0 + 2\Omega_{\Lambda 0}) \right]; \quad (29)$$

$\Lambda \sim H^2$ :

$$\dot{S}^2 = H_0^2 S_0^2 \left[ \frac{\Omega_0 - 2\Omega_{\Lambda 0}}{1 - 3\Omega_{\Lambda 0}} \left( \frac{S_0}{S} \right)^{1-3\Omega_{\Lambda 0}} + \frac{1 - \Omega_0 - \Omega_{\Lambda 0}}{1 - 3\Omega_{\Lambda 0}} \right]; \quad (30)$$

$\Lambda \sim \rho$ :

$$\dot{S}^2 = H_0^2 S_0^2 \left[ (\Omega_0 + \Omega_{\Lambda 0}) \left( \frac{S_0}{S} \right)^{(\Omega_0 - 2\Omega_{\Lambda 0})/(\Omega_0 + \Omega_{\Lambda 0})} + 1 - \Omega_0 - \Omega_{\Lambda 0} \right]. \quad (31)$$

It is now clear from equations (29)-(31) that the dynamics of the models depend only on the values of  $\Omega_0$  and  $\Omega_{\Lambda 0}$ . Also the relative behaviour of  $S$  from these equations is quite arbitrary and changes with different pairs of  $\Omega_0$  and  $\Omega_{\Lambda 0}$ . It thus seems that in general there is no feature which distinguishes the models. We also note that for  $\Omega_0 = 2\Omega_{\Lambda 0}$ , the models become identical reducing to  $S \sim t$  and  $\rho \sim \Lambda \sim t^{-2}$ . Also, for the trivial case  $\Lambda = 0$ , the models become identical reducing, obviously, to the standard FRW models with zero  $\Lambda$ .

We shall now derive the  $m$ - $z$  and  $\Theta$ - $z$  relations in the models in order to compare them with observations, which will be done in the following sections.

### 3. Study of magnitude-redshift relation in the models

Suppose that the observer at  $r = 0$  and  $t = t_0$  receives the light emitted at  $t = t_1$  from a source of absolute luminosity  $L$  located at a radial distance  $r_1$ . The cosmological redshift  $z$  of the source is related with  $t_1$  and  $t_0$  by  $1 + z = S(t_0)/S(t_1)$ . If the (apparent) luminosity of the source measured by the observer is  $l$ , the *luminosity distance*  $d_L$  of the source, defined by

$$l \equiv \frac{L}{4\pi d_L^2}, \quad (32)$$

is then given by

$$d_L = (1+z)S_0 r_1. \quad (33)$$

For historical reasons, the absolute and apparent luminosities  $L$  and  $l$  are defined, respectively, in terms of the absolute and apparent magnitudes  $M$  and  $m$  as  $L = 10^{-2M/5} \times 3.02 \times 10^{35} \text{ erg s}^{-1}$  and  $l = 10^{-2m/5} \times 2.52 \times 10^{-5} \text{ erg cm}^{-2} \text{ s}^{-1}$  (Weinberg 1972). When written in terms of  $M$  and  $m$ , equation (32) yields

$$m(z; \mathcal{M}, \Omega_0, \Omega_{\Lambda 0}) = \mathcal{M} + 5 \log_{10} \left[ \frac{\mathcal{D}_L(z; \Omega_0, \Omega_{\Lambda 0})}{1 \text{Mpc}} \right], \quad (34)$$

where  $\mathcal{M} \equiv M - 5 \log_{10} H_0 + 25$  and  $\mathcal{D}_L(z; \Omega_0, \Omega_{\Lambda 0}) \equiv H_0 d_L(z; \Omega_0, \Omega_{\Lambda 0}, H_0)$  is the dimensionless *luminosity distance*. By using equation (3), the coordinate distance  $r_1$ , appearing in equation (33), yields

$$\psi(r_1) = \int_{S_0/(1+z)}^{S_0} \frac{dS}{S\dot{S}} \quad (35)$$

with

$$\begin{aligned} \psi(r_1) &= \sin^{-1} r_1, & k &= 1 \\ &= r_1, & k &= 0 \\ &= \sinh^{-1} r_1, & k &= -1. \end{aligned} \quad (36)$$

The *luminosity distances* for the different models, described for the cases (1), (2) and (3), will be given by calculating the right hand side of equation (35) for these models. By using equations (29)-(31), equation (35) can be written, for the three models, as

$$\psi(r_1) = \frac{1}{S_0 H_0} I_j, \quad (37)$$

where  $I_j$  ( $j = 1, 2$  and  $3$  correspond to, respectively, the three models described for the cases (1), (2) and (3)) is given by

$$I_1 = \int_0^z [(2\Omega_{\Lambda 0} - \Omega_0 + 1)(1+z')^2 - (2\Omega_{\Lambda 0} - \Omega_0)(1+z')^3]^{-1/2} dz', \quad (38)$$

$$I_2 = \int_0^z \left[ \frac{(\Omega_0 - 2\Omega_{\Lambda 0})}{(1 - 3\Omega_{\Lambda 0})} (1 + z')^{3(1 - \Omega_{\Lambda 0})} + \frac{(1 - \Omega_0 - \Omega_{\Lambda 0})}{(1 - 3\Omega_{\Lambda 0})} (1 + z')^2 \right]^{-1/2} dz' \quad (39)$$

and

$$I_3 = \int_0^z [(\Omega_0 + \Omega_{\Lambda 0})(1 + z')^{3\Omega_0/(\Omega_0 + \Omega_{\Lambda 0})} + (1 - \Omega_0 - \Omega_{\Lambda 0})(1 + z')^2]^{-1/2} dz'. \quad (40)$$

(For convenience, we also write the similar integral  $I_c$  for the constant  $\Lambda$ -Friedmann models obtained as

$$I_c = \int_0^z [(1 + \Omega_0 z')(1 + z')^2 - z'(2 + z')\Omega_{\Lambda 0}]^{-1/2} dz',$$

which will be used to compare our results with those for the constant  $\Lambda$ -models.)

Equations (33), (36) and (37) can also be combined into a single compact equation to give

$$\mathcal{D}_L(z; \Omega_0, \Omega_{\Lambda 0}) = \frac{(1 + z)}{\sqrt{\mathcal{K}}} \xi(\sqrt{\mathcal{K}} I_j), \quad (41)$$

where

$$\begin{aligned} \xi(x) &= \sin(x) \text{ with } \mathcal{K} = \Omega_{k0} \text{ when } \Omega_{k0} > 0, \\ \xi(x) &= \sinh(x) \text{ with } \mathcal{K} = -\Omega_{k0} \text{ when } \Omega_{k0} < 0 \text{ and} \\ \xi(x) &= x \text{ with } \mathcal{K} = 1 \text{ when } \Omega_{k0} = 0. \end{aligned}$$

Thus for given  $\mathcal{M}$ ,  $\Omega_0$  and  $\Omega_{\Lambda 0}$ , equations (34) and (41) give the predicted value of  $m(z)$  at a given  $z$ . Using the observed values of the effective magnitude  $m_i^{\text{eff}}$  (corrected for the width-luminosity relation) and the same standard errors  $\sigma_{z,i}$  and  $\sigma_{m_i^{\text{eff}}}$  of the  $i$ th supernova with redshift  $z_i$  as used by Perlmutter et al, we compute  $\chi^2$  according to

$$\chi^2 = \sum_{i=1}^{54} \frac{[m_i^{\text{eff}} - m(z_i)]^2}{(\sigma_{z,i}^2 + \sigma_{m_i^{\text{eff}}}^2)}. \quad (42)$$

The best fit parameters are obtained by minimizing this equation.

We consider the data set on  $m^{\text{eff}}$  and  $z$  of 54 supernovae as used by Perlmutter et al in their primary fit C. This set comprises 38 high-redshift

supernovae from the Supernova Cosmology Project (excluding 2 outliers and 2 likely reddened ones from the full sample of 42 supernovae) together with 16 low-redshift supernovae from the Calan-Tololo sample (excluding 2 outliers from the full sample of 18 supernovae). We fit the low- and high-redshift supernovae simultaneously to equation (34) to estimate the parameters  $\mathcal{M}$ ,  $\Omega_0$  and  $\Omega_{\Lambda 0}$ . This fitting procedure is followed by Perlmutter et al in their primary fit C. We have listed the best-fit values in Table 1. The global best-fit parameters have been calculated by giving free rein to  $\Omega_0$ ,  $\Omega_{\Lambda 0}$  and  $\mathcal{M}$ , i.e., at  $54 - 3 = 51$  degrees of freedom (dof) whereas the best-fit parameters for flat models are calculated at 52 degrees of freedom with the constraint  $\Omega_0 + \Omega_{\Lambda 0} = 1$ . For comparison, we have shown the best-fit parameters for the constant  $\Lambda$ -models. The  $\chi^2$  values obtained at different degrees of freedom have also been converted into confidence levels (cl) [the goodness of fit probability  $Q = 1 - \text{cl}\%$ ]. In Figure 1, we have shown the fit of the data to the best-fitting flat models and compared it with the fit of the data to the Einstein-de Sitter model.

It may be mentioned that Perlmutter et al have also fitted the data for only 3 parameters  $\mathcal{M}$ ,  $\Omega_0$  and  $\Omega_{\Lambda 0}$  and not for the 4 parameters  $\mathcal{M}$ ,  $\Omega_0$ ,  $\Omega_{\Lambda 0}$  and  $\alpha$  (the slope of the width-luminosity relation) as mentioned in their paper (from a personal discussion with Professor R. S. Ellis, one of the authors of the paper). A self-consistent 4-parameter fit has been done by Efstathiou et al (1999).

**Table 1.** Best-fit values of different parameters for three variable  $\Lambda$ -models estimated from the Type Ia supernovae data. For comparison, the best-fit parameters for the constant  $\Lambda$ -Friedmann model (Perlmutter et al') and Einstein-de Sitter model have also been shown.

Models	Best-Fit Parameters (Flat models)					Global Best-Fit Parameters					
	$\Omega_0$	$\mathcal{M}$	$\chi^2$	dof	cl(%)	$\Omega_0$	$\Omega_{\Lambda 0}$	$\mathcal{M}$	$\chi^2$	dof	cl(%)
$\Lambda \sim S^{-2}$	0.49	23.97	58.97	52	76	1.86	1.52	23.95	57.43	51	75
$\Lambda \sim H^2$	0.4	23.96	58.33	52	75	0.98	1.53	23.91	56.86	51	73
$\Lambda \sim \rho$	0.4	23.96	58.33	52	75	1.62	1.59	23.93	56.91	51	74
$\Lambda = \text{const}$	0.28	23.94	57.68	52	73	0.79	1.41	23.91	56.82	51	73
$\Lambda = 0,$ $\Omega = 1$		24.21	92.89	53	99.9						

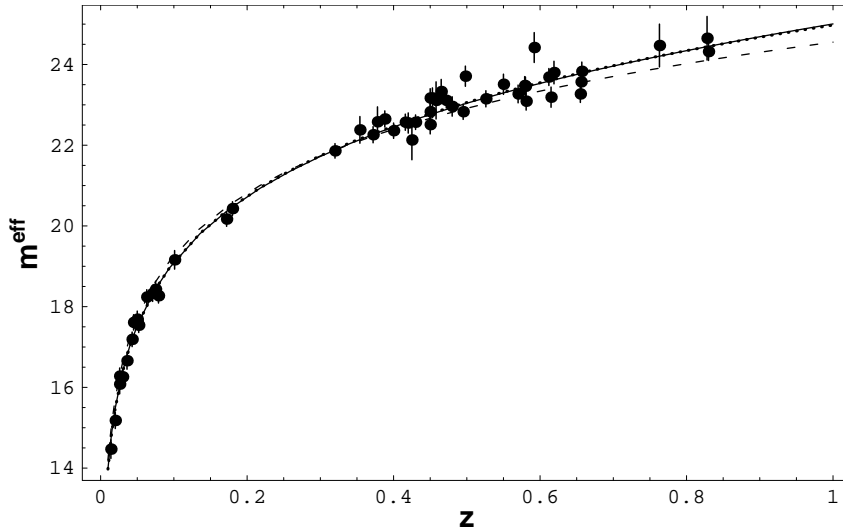


**Figure 1.** Hubble diagrams for 38 high-redshift and 16 low-redshift supernovae are shown. The solid curve represents the best-fitting flat model  $\Omega_0 = 0.49$  (for  $\Lambda \sim S^{-2}$ ) and the dotted curve represents the best-fitting flat model  $\Omega_0 = 0.4$  (for  $\Lambda \sim H^2$ ). The curves overlap on each other because of the same goodness of fit. For comparison, the canonical Einstein-de Sitter model ( $\Omega_k = 0$ ,  $\Omega_\Lambda = 0$ ) has also been plotted (dashed curve).

The fits of the data to all the three variable  $\Lambda$ -models are almost as good as to the constant  $\Lambda$ -Friedmann model (Perlmutter et al') with  $\chi^2/\text{dof} \approx 1$  (a very good fit indeed) and require non-zero, positive values of  $\Lambda$ . It is clear from Table 1 and Figure 1 that the data do not fit the Einstein-de Sitter model ( $\Omega = 1$ ,  $\Lambda = 0$ ). We note that the global best-fit values for  $\Omega_0$  and  $\Omega_{\Lambda 0}$  are always larger than those for the corresponding flat models. Also the estimates of  $\Omega_0$  for the variable  $\Lambda$ -models are always higher than that for the constant  $\Lambda$ -Friedmann model (Perlmutter et al') and hence require dark matter, though not as much as in the non-flat models. It is also clear from the Table that for all the three variable  $\Lambda$ -models,  $\Omega_0/2$  is less than the corresponding  $\Omega_{\Lambda 0}$  (as is the case for the constant  $\Lambda$ -Perlmutter et al' model) leading to  $q_0 < 0$ .

One may notice that the estimates of the parameters for the flat models for the cases  $\Lambda \sim H^2$  and  $\Lambda \sim \rho$  are exactly same. This simply reveals the fact that for  $k = 0$ , the two models become identical. This can be checked from equations (17) and (18) which, for  $k = 0$ , give  $S \sim t^{2(1+n)/3(1+w)}$  leading to  $\Lambda \sim \rho \sim t^{-2} \sim H^2$ . This may be considered as a cross check for our fitting procedure.

Elsewhere (Vishwakarma 2000a) we have used this data set with a different fitting procedure for the model  $\Lambda \sim S^{-2}$ . Instead of fitting the high and low-redshift data simultaneously, we used low-redshift measurements to determine  $\mathcal{M}$  and by using this value in equation (34) we performed a two-parameter fit of the high-redshift supernovae to estimate  $\Omega_0$  and  $\Omega_{\Lambda 0}$ . The best-fit values so obtained are in good agreement with the estimates shown in Table 1 for that model.

We would like to mention that the supernovae data have also been used in many studies to place constraints on models with ‘x-fluid’ ( $p_x = w\rho_x$  with  $-1 < w < 0$ ) or ‘quintessence’ (a slowly varying scalar field) (Waga and Miceli 1998; Efstathiou 1999; Perlmutter, Turner and White 1999; Podariu and Ratra 1999; and the references therein). Though ‘x-fluid’ and ‘quintessence’ are formally equivalent to a variable  $\Lambda$ , however, these models are essentially different from our kinematical ‘usual’  $\Lambda$ -models considered in this paper in the sense that in our models matter is created as a result of the decaying  $\Lambda$ , as has been mentioned in section 2, whereas in the exotic fluid description, the exotic component is conserved. In the present approach (or in the case of ‘x-fluid’ with  $w = -1$ ), if the  $\Lambda$ -source  $[\{\Lambda(t)/8\pi G\}g_{ij}]$  is conserved separately, then  $\Lambda$  would become constant, as has been mentioned earlier.

#### 4. Study of angular size-redshift relation in the models

The compact radio sources, of angular size of the order of a few milliarcseconds, which are observed with very long baseline interferometry (VLBI), are deeply embedded in the galactic nuclei and are expected to be free from the evolutionary effects. These sources are attractive for the test of cosmological models because they are usually identified with quasars which, in general, have high redshifts, so the differences between models may be more easily distinguished than for the extended double-lobed sources.

Kellermann (1993) used a sample of 79 such sources and showed that a

credible  $\Theta$ - $z$  relation can emerge. His main motivation was, however, limited to showing that the resulting  $\Theta$ - $z$  diagram was cosmologically credible and compatible with the Einstein-de Sitter canonical model with  $\Lambda = 0$  rather than to be specific about the acceptable ranges for the various cosmological parameters. Extending his work, by introducing  $\Lambda$  into the picture, Jackson and Dodgson (1996) showed that the Kellermann's data could also fit very well with a low density, highly decelerating model having a large negative cosmological constant. Later on, a more extensive exercise was carried out by Jackson and Dodgson (1997) by considering a bigger sample of 256 ultra-compact sources selected from the compilation from Gurvits (1994). Then, they concluded that the canonical cold dark matter model with  $\Lambda = 0$  was ruled out by the observed relationship at 98.5 percent level of confidence and low density FLRW models with either sign of  $\Lambda$  were favoured. Elsewhere we (Vishwakarma 2000b) used the data set from Jackson and Dodgson (1997) in the model resulting from the case (3) and found the model in good agreement with the data.

Recently this data set has been updated and extended by Gurvits et al (1999) as a sample of 330 sources (though at the expense of homogeneity) distributed over a wide range of redshifts  $0.011 \leq z \leq 4.72$ . In order to minimize any possible dependence of linear size on luminosity and that of angular size on spectral index, they discarded lower values of luminosities and extreme values of spectral indices and selected only 145 sources with total radio luminosity  $Lh^2 \geq 10^{26}$  W/Hz and  $-0.38 \leq$  spectral index  $\leq 0.18$ , which are hoped to be free from the evolutionary effects and hence conceivably comprise a set of standard objects. This sub-sample was distributed into 12 bins, each bin containing 12-13 sources. They studied the  $\Theta$ - $z$  relation in Friedmann models with  $\Lambda = 0$  for this sample and found the best-fit model as  $q_0 = 0.21$  with no-evolution assumption. However, as we shall see, the models with a non-zero  $\Lambda$  (constant) are also in good agreement (even better) with the data. We shall also use this data set to study the  $\Theta$ - $z$  relation in the variable- $\Lambda$  models considered in this paper. For this purpose, we now derive the  $\Theta$ - $z$  relation in the models by assuming that there are no evolutionary effects due to a linear size-luminosity or linear size-redshift dependence.

The *angular diameter distance*  $d_A$  of a light source of linear size  $d$  and angular size  $\Theta$ , defined by

$$d_A = \frac{d}{\Theta}, \quad (43)$$

is related to the *luminosity distance*  $d_L$  of the source by

$$d_A = \frac{d_L}{(1+z)^2}. \quad (44)$$

By comparing this with equation (33) and using (36), (37) and (43), we obtain the  $\Theta$ - $z$  relation in the models as

$$\Theta(z; dh, \Omega_0, \Omega_{\Lambda 0}) = \left(100 \text{ km s}^{-1} \text{Mpc}^{-1}\right) dh \sqrt{\mathcal{K}} (1+z) / \xi(\sqrt{\mathcal{K}} I_j), \quad (45)$$

where  $h$  is the present value of the Hubble parameter in units of  $100 \text{ km s}^{-1} \text{Mpc}^{-1}$ .

It is thus clear that for given  $dh$ ,  $\Omega_0$  and  $\Omega_{\Lambda 0}$ , the predicted value  $\Theta(z)$ , at a given  $z$ , is completely determined. Using median values of the grouped data into 12 bins, as used by Gurvits et al, we calculate the theoretical  $\Theta(z)$  for a wide range of parameters  $dh$ ,  $\Omega_0$  and  $\Omega_{\Lambda 0}$  and compute  $\chi^2$  according to

$$\chi^2 = \sum_{i=1}^{12} \left[ \frac{\Theta_i - \Theta(z_i)}{\sigma_i} \right]^2, \quad (46)$$

which measures the agreement between the theoretical  $\Theta(z)$  and the observed value  $\Theta_i$  with the errors  $\sigma_i$  of the  $i$ th bin in the sample. The maximum likelihood estimates of the parameters are obtained by minimizing  $\chi^2$  as usual. We have listed our results in Table 2 below.

**Table 2.** Best-fit parameters for the Friedmann model (with constant  $\Lambda$ ) and three variable  $\Lambda$ -models estimated from Gurvits et al' data. For comparison, the best-fit parameters for Gurvits et al' model have also been shown. (The values of  $dh$  are shown in unit of 1 pc.)

Models	Best-Fit Parameters (Flat models)					Global Best-Fit Parameters					
	$\Omega_0$	$dh$	$\chi^2$	dof	cl(%)	$\Omega_0$	$\Omega_{\Lambda 0}$	$dh$	$\chi^2$	dof	cl(%)
$\Lambda \sim S^{-2}$	0.68	18.25	4.71	10	9	0.97	0.61	17.99	4.66	9	14
$\Lambda \sim H^2$	0.67	18.53	4.72	10	9	0.29	1.03	23.71	4.28	9	11
$\Lambda \sim \rho$	0.67	18.53	4.72	10	9	0.53	0.82	22.41	4.27	9	11
$\Lambda = \text{const}$	0.2	22.29	4.52	10	8	0.08	1.16	27.73	4.17	9	10
Gurvits's model						0.43	0	17.72	4.74	10	9

We thus find that the Gurvits et al' model (Friedmann model with a vanishing  $\Lambda$ ) is not the best-fitting model. The best-fitting model with constant  $\Lambda$  is a low-density model dominated by positive  $\Lambda$ . It is clear from Table 2 that all the models, variable- or constant- $\Lambda$ , show an excellent fit to the data with  $\chi^2/\text{dof} \approx 0.5$  and require non-zero, positive values of  $\Lambda$ . Here again the best-fit values of  $\Omega_0$  for variable  $\Lambda$ -models are larger than the best-fit  $\Omega_0$  for the constant  $\Lambda$ -model. Unlike the supernovae data, this data set requires both, the accelerating and decelerating models: the global best-fit parameters (for the variable as well as the constant  $\Lambda$ -models) represent an accelerating expansion whereas the best-fit parameters for the flat models (only the variable  $\Lambda$ -ones) represent a decelerating expansion.

Once again we encounter with the same values of the parameters for the models  $\Lambda \sim H^2$  and  $\Lambda \sim \rho$  for the flat cases, which serves a cross check for the fitting procedure. In Figure 2, we have shown the fit of the data to the flat models.

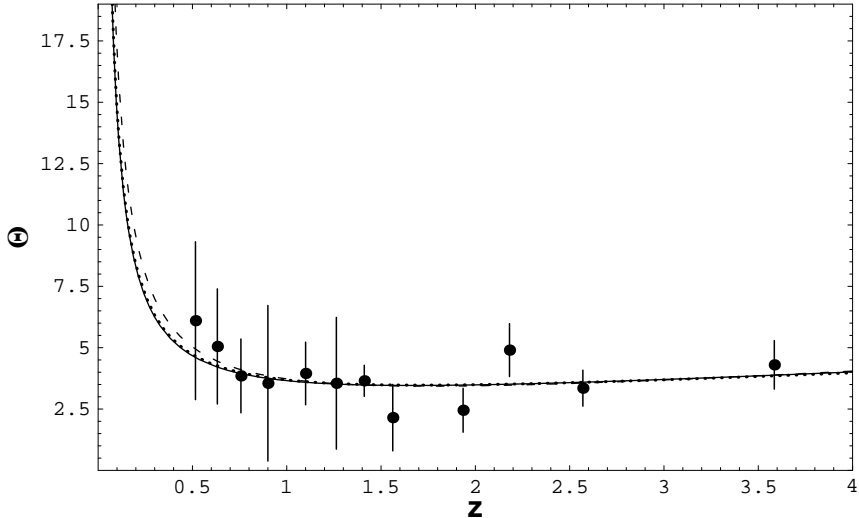


**Figure 2.** Gurvits et al’ data points are compared with the three best-fitting flat models obtained for the cases:  $\Lambda \sim S^{-2}$  with  $\Omega_0 = 0.68$  (solid curve),  $\Lambda \sim H^2$  with  $\Omega_0 = 0.67$  (dotted curve) and  $\Lambda = \text{constant}$  with  $\Omega_0 = 0.2$  (dashed curve).

Following Gurvits et al, it would be worth while to study the consequences if the source linear size depends on the source luminosity and redshift (i.e., the sources are not the ‘true’ standard rods). For this purpose, we consider the following phenomenological expression for  $\Theta$  as has been considered by Gurvits et al:

$$\Theta \equiv d/d_A \sim \ell h L^\beta (1+z)^\gamma \mathcal{D}_A^{-1}, \quad (47)$$

where  $\mathcal{D}_A \equiv H_0 d_A$  is the dimensionless *angular diameter distance* and  $\ell h$  is the linear size scaling factor which reduces to  $dh$  for the no-evolution case. The parameters  $\beta$  and  $\gamma$ , representing the dependence of the linear size on the source luminosity and redshift respectively, are to be estimated from the data. We fit the Gurvits et al’ sub-sample to equation (47) for five parameters  $\Omega_0$ ,  $\Omega_{\Lambda 0}$ ,  $\ell h$ ,  $\beta$  and  $\gamma$ . The best-fit values for the three models are obtained as follows.

$\Lambda \sim S^{-2}$ :

$$\Omega_0 = 0.89, \quad \Omega_{\Lambda 0} = 0.58, \quad lh = 23.69, \quad \beta = 0.37, \quad \gamma = -0.45, \quad \chi^2 = 3.21;$$

$\Lambda \sim H^2$ :

$$\Omega_0 = 0.39, \quad \Omega_{\Lambda 0} = 0.95, \quad lh = 28.16, \quad \beta = 0.37, \quad \gamma = -0.44, \quad \chi^2 = 2.72;$$

$\Lambda \sim \rho$ :

$$\Omega_0 = 0.51, \quad \Omega_{\Lambda 0} = 0.83, \quad lh = 17.9, \quad \beta = 0.38, \quad \gamma = -0.42, \quad \chi^2 = 2.47.$$

We find that the estimates of  $\Omega_0$  and  $\Omega_{\Lambda 0}$  thus obtained are in agreement with those shown in Table 2. The estimates of  $\beta$  and  $\gamma$  are in qualitative agreement with  $\beta = 0.37$  and  $\gamma = -0.58$  obtained by Gurvits et al. The values of  $\Omega_0$  and  $\Omega_{\Lambda 0}$  for the case  $\Lambda \sim \rho$  are also in qualitative agreement with the estimates of these parameters obtained (by assuming no-evolution) from an independent sample of sources (Vishwakarma 2000b). It thus seems that there is no need to consider evolutionary effects due to linear size-luminosity or linear size-redshift dependence. However, this result, which is based on the above-made comparisons, is rather superficial than indicative because there are large uncertainties in the above-mentioned estimates which are due to the large number of regression parameters.

## 5. Conclusion

We find that all the variable  $\Lambda$ -models, fit the data sets equally well and a discrimination between the different dynamical laws or between the different geometries is not possible with the present status of the data sets. While the fit of the models (constant, as well as, variable  $\Lambda$ ) to the supernovae data is very good with  $\chi^2/\text{dof} \approx 1$ , their fit to the radio sources data is excellent with  $\chi^2/\text{dof}$  even less than 1. The estimates of the density parameter  $\Omega_0$  (from both data sets) for the variable  $\Lambda$ -models are found higher than those for the constant  $\Lambda$ -Friedmann model. The supernovae data set requires an accelerating expansion for the variable  $\Lambda$ -models as it does for the constant  $\Lambda$ -model. However, the radio sources data set requires accelerating as well as decelerating expansion for the variable  $\Lambda$ -models, though only an accelerating expansion for the constant  $\Lambda$ -model.

Many of the  $\Omega_0$  values shown in Tables 1 and 2 (especially the global best-fit estimates from the supernovae data) are found rather high. In view of the

small observed value of  $\Omega_0$ , this implies that not all the best-fit solutions found here are realistic. For  $0.2 < \sim \Omega_0 < \sim 0.5$ , which seems to be the general consensus at present, the only realistic solutions are (a) estimated from the supernovae data: the best-fit solutions for flat models (including the constant  $\Lambda$ -case); (b) estimated from the radio sources data: the global best-fit solutions for the models  $\Lambda \sim H^2$  and  $\Lambda \sim \rho$ , the best-fit solution for the flat model with  $\Lambda = \text{constant}$  and the Gurvits et al' model.

As in the case of the recent analyses of the CMB results from BOOMERANG and MAXIMA (Jaffe et al, 2000), our global best fit values from both data sets imply a spherical universe ( $\Omega_0 + \Omega_{\Lambda 0} > 1$ ).

One may notice from Tables 1 and 2 that the best-fit values of  $\Omega_0$  and  $\Omega_{\Lambda 0}$  from the two data sets are a bit too different for the corresponding models, especially in the non-flat cases. The reason for this may be the incomplete understanding of a number of astrophysical effects and processes (evolution, inter galactic dust, etc.). It should also be noted that the Gurvits et al' compilation is based on very inhomogeneous data obtained by many different observers using different instruments and imaging techniques. New VLBI observations now in progress will improve the accuracy of the observed  $\Theta - z$  relations as it will provide a uniform data set for analysis. A reasonable hope is that, as the data accumulates and its understanding improves, such tests coupled with plausible evolutionary hypothesis will lead to similar results. These results should be consistent with the CMB measurements and also with the spatial scale of the peak in the power spectrum of galaxy perturbations which provides a standard ruler in co-moving space for measuring cosmological parameters (Broadhurst and Jaffe 2000, Roukema and Mamon 2000).

### Acknowledgments

The author thanks Professors J V Narlikar and R S Ellis for fruitful discussions and the Department of Atomic energy, India for support available in conjunction with the Homi Bhabha Professorship of Professor J V Narlikar. Thanks are also due to Dr. L I Gurvits for sending his compilation.

### References:

- Abdel-Rahaman A-M M 1992 Phys. Rev. D **45** 3492  
 Abdussattar and Vishwakarma R G 1996 Pramana - J. Phys **47** 41  
 \_\_\_\_\_ 1997 Class. Quantum Grav. **14** 945

Arbab A I and Abdel-Rahaman A-M M 1994 Phys. Rev. D **50** 7725  
 Arbab A I 1997 Gen. Relativ. Grav. **29** 61  
 Beesham A 1994 Gen. Relativ. Grav. **26** 159  
 Berman M S 1991 Phys. Rev. D **43** 1075  
 Berman M S and Som M M 1990 Int. J. Theor. Phys. **29** 1411  
 Bertolami O 1986 Nuovo Cimento B **93** 36  
 Broadhurst T and Jaffe A H 1999 Preprint (astro-ph/9904348), (in press  
 with ApJL)  
 Carroll S M Press W H and Turner E L 1992 Ann. Rev. Astron.  
 Astrophys. **30** 499  
 Carvalho J C Lima J A S and Waga I 1992 Phys. Rev. D **46** 2404  
 Chen W and Wu Y S 1990 Phys. Rev. D **41** 695  
 Efstathiou G Bridle S L Lasenby A N Hobson M P and Ellis R S 1999  
 MNRAS **303** L47  
 Efstathiou G 1999 Preprint (astro-ph/9904356)  
 Endo M and Fukui T 1977 Gen. Relativ. Grav. **8** 833  
 Garnavich et al 1998 Astrophys. J. **509** 74  
 Gurvits L I 1994 Astrophys. J. **425** 442  
 Gurvits L I Kellermann K I and Frey S 1999 Astron. Astrophys. **342** 378  
 Jackson J C and Dodgson M 1996 MNRAS **278** 603  
 \_\_\_\_\_ 1997 MNRAS **285** 806  
 Jaffe et al 2000 Preprint (astro-ph/0007333)  
 Kellermann K I 1993 Nat. **361** 134  
 Lau Y K 1985 Aust. J. Phys. **38** 547  
 Lima J A S and Carvalho J C 1994 Gen. Relativ. Grav. **26** 909  
 Lopez J L and Nanopoulos D V 1996 Mod. Phys. Lett. A **11** 1  
 Overduin J M and Cooperstock F I 1998 Phys. Rev. D **58** 043506  
 Ozer M and Taha M O 1987 Nucl. Phys. B **287** 776  
 Perlmutter S et al 1999 Astrophys. J. **517** 565  
 Perlmutter S, Turner M S and White M 1999 Preprint (astro-ph/9901052)  
 Podariu S and Ratra B 1999 Preprint (astro-ph/9910527)  
 Riess A G et al 1998 Astron. J. **116** 1009  
 Roukema B F and Mamon G A 2000 Astron. Astrophys. **358** 395  
 Sahni V and Starobinsky A 2000 Int. J. Mod. Phys. D **9** 373  
 Salim L M and Waga I 1993 Class. Quantum Grav. **10** 1767  
 Turner M S and White M 1997 Phys. Rev. D **56** 4439  
 Vilenkin A 1985 Phys. Rep. **121** 265

Vishwakarma R G 1999 Preprint (gr-qc/9912106)  
\_\_\_\_\_ 2000a submitted  
\_\_\_\_\_ 2000b Class. Quantum Grav. **17** 3833 (gr-qc/9912105)  
Waga I 1993 Astrophys. J. **414** 436  
Waga I and Miceli 1998 Preprint (astro-ph/9811460)  
Weinberg S 1972 Gravitation and Cosmology, John Wiley  
\_\_\_\_\_ 1989 Rev. Mod. Phys. **61** 1  
Wetterich C 1995 Astron. Astrophys. **301** 321  
Zlatev I, Waga I and Steinhardt P J 1999 Phys. Rev. Lett. **82** 896